

Direct Sugar Binding to LacY Measured by Resonance Energy Transfer<sup>†</sup>

Irina N. Smirnova, Vladimir N. Kasho, and H. Ronald Kaback\*

Department of Physiology and Microbiology, Immunology &amp; Molecular Genetics, Molecular Biology Institute, University of California Los Angeles, Los Angeles, California 90095-7327

Received August 10, 2006; Revised Manuscript Received October 13, 2006

**ABSTRACT:** Trp151 in the lactose permease of *Escherichia coli* (LacY) is an important component of the sugar-binding site and the only Trp residue out of six that is in close proximity to the galactopyranoside in the structure (1PV7). The short distance between Trp151 and the sugar is favorable for Förster resonance energy transfer (FRET) to nitrophenyl or dansyl derivatives with the fluorophore at the anomeric position of galactose. Modeling of 4-nitrophenyl- $\alpha$ -D-galactopyranoside ( $\alpha$ -NPG) in the binding-site of LacY places the nitrophenyl moiety about 12 Å away from Trp151, a distance commensurate with the Förster distance for a Trp–nitrobenzoyl pair. We demonstrate here that  $\alpha$ -NPG binding to LacY containing all six native Trp residues causes galactopyranoside-specific FRET from Trp151. Moreover, binding of  $\alpha$ -NPG is sufficiently slow to resolve time-dependent fluorescence changes by stopped-flow. The rate of change in Trp  $\rightarrow$   $\alpha$ -NPG FRET is linearly dependent upon sugar concentration, which allows estimation of kinetic parameters for binding. Furthermore, 2-(4'-maleimidylanilino)naphthalene-6-sulfonic acid (MIANS) covalently attached to the cytoplasmic end of helix X is sensitive to sugar binding, reflecting a ligand-induced conformational change. Stopped-flow kinetics of Trp  $\rightarrow$   $\alpha$ -NPG FRET and sugar-induced changes in MIANS fluorescence in the same protein reveal a two-step process: a relatively rapid binding step detected by Trp151  $\rightarrow$   $\alpha$ -NPG FRET followed by a slower conformational change detected by a change in MIANS fluorescence.

The lactose permease of *Escherichia coli* (LacY),<sup>1</sup> a member of the major facilitator superfamily (1), is arguably the most intensively studied membrane transport protein (2, 3) and one of few with a known crystal structure (4). A proposed mechanism for lactose transport (3) includes ordered binding of an H<sup>+</sup> and a galactopyranoside on one side of the membrane followed by a conformational change and ordered release of the sugar and the H<sup>+</sup> on the opposite side. Although the X-ray structure of LacY reveals an inward-facing conformation, there is a body of data (3) supporting the concept that the transport cycle includes widespread conformational changes linked to the binding and release of sugar. Therefore, knowledge regarding individual steps in the transport mechanism is paramount to understanding the overall mechanism.

Only a handful of side chains are essential for sugar recognition and binding (Figure 1B). Arg144 (helix V) forms a bidentate H-bond with the O<sub>4</sub> and O<sub>3</sub> atoms of the galactopyranosyl ring (4), confirming the critical role of this

residue in sugar binding and recognition (3). Glu126 (helix IV), another important residue for binding, is in close proximity to Arg144 and may interact with the O<sub>4</sub>, O<sub>5</sub>, or O<sub>6</sub> atoms of the galactopyranosyl ring via water molecules. An aromatic residue at position 151 (helix V), preferably Trp, is irreplaceable for sugar binding (5), stacking hydrophobically with the galactopyranosyl ring (6, 7). Glu269 (helix VIII) in the C-terminal domain, which is also involved in H<sup>+</sup> translocation, may interact with the O<sub>3</sub> atom of the galactopyranosyl ring, forms a salt bridge with Arg144 and is in close proximity to Trp151 (4, 7–9).

Detection and quantification of sugar binding can be accomplished by flow dialysis or substrate protection against alkylation of Cys148 with maleimides (10–16). Cys148 is near the sugar-binding site in LacY, and sugar binding sterically blocks alkylation. Each of these techniques is a steady-state measurement and involves use of radioactivity or fluorescence. Binding can also be detected and quantified by ligand-induced changes in the fluorescence of 2-(4'-maleimidylanilino)naphthalene-6-sulfonic acid (MIANS) with purified single-Cys V331C. In this case, the fluorophore is positioned far from the sugar binding site and reflects a long-range conformational change resulting from sugar binding (11, 14, 15, 17). However, none of the methods have been used to measure kinetic parameters.

In this paper, we describe a novel method for determining and quantifying sugar binding by using the intrinsic Trp fluorescence of purified LacY. Formation of a donor–acceptor pair between Trp151 and  $\alpha$ -NPG or 6'-(N-dansyl)-aminoethyl-1-thio- $\beta$ -D-galactopyranoside (Dns<sup>6</sup>Gal) in the sugar-binding site results in Förster resonance energy transfer

<sup>†</sup> This work was supported by NIH grants DK051131 and DK069463 to H.R.K.

\* Corresponding author. Mailing address: Department of Physiology, UCLA, MacDonald Research Laboratories, Los Angeles, CA 90095-7327. Telephone: (310) 206-5053. Fax: (310) 206-8623. E-mail: RKABACK@Mednet.UCLA.edu.

<sup>1</sup> Abbreviations: LacY, lactose/H<sup>+</sup> symporter from *Escherichia coli*; DDM, dodecyl- $\beta$ -D-maltopyranoside; TDG,  $\beta$ -D-galactopyranosyl-1-thio- $\beta$ -D-galactopyranoside;  $\alpha$ -NPG, 4-nitrophenyl- $\alpha$ -D-galactopyranoside; *ortho*-NPG, 2-nitrophenyl- $\alpha$ -D-galactopyranoside; NPGlc, 4-nitrophenyl- $\alpha$ -D-glucopyranoside; Dns<sup>6</sup>Gal, 6'-(N-dansyl)aminoethyl-1-thio- $\beta$ -D-galactopyranoside; MIANS, 2-(4'-maleimidylanilino)naphthalene-6-sulfonic acid (sodium salt); FRET, Förster resonance energy transfer; R<sub>0</sub>, Förster distance.

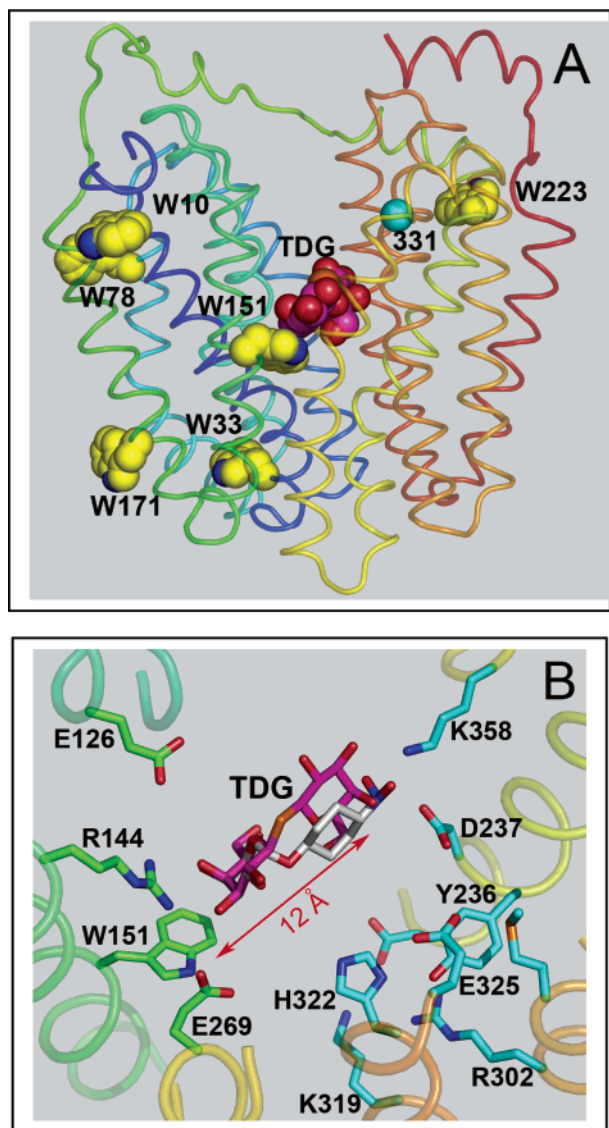


FIGURE 1: Location of Trp residues in the structure of C154G LacY with bound sugar (1PVG). The structures are displayed with Pymol 0.98 (DeLano Scientific LLC, Inc.), and transmembrane helices are colored from blue (helix I) to red (helix XII). (A) Overall structure of LacY with all native Trp residues shown as yellow spheres and bound TDG shown as pink spheres. A cyan sphere highlights the C $\alpha$  atom of position 331. (B) Modeling of bound  $\alpha$ -NPG. Amino acid residues involved in substrate binding and proton translocation (Glu269 is involved in both) are shown in green and cyan sticks, respectively. Bound TDG is shown as pink sticks, and the position of the nitrophenyl moiety in  $\alpha$ -NPG is shown as gray sticks.

(FRET), which can be measured in the steady-state or by stopped-flow. In addition, the time course of a ligand-induced conformational change is measured with MIANS-labeled V331C LacY. The results are consistent with a mechanism in which a relatively rapid sugar-binding step is followed by a slower conformational change.

## EXPERIMENTAL PROCEDURES

**Materials.** Oligonucleotides were synthesized by Integrated DNA Technologies, Inc. (Coralville, IA). Restriction enzymes were purchased from New England Biolabs (Beverly, MA). The QuickChange II kit was from Stratagene (La Jolla, CA). Dns<sup>6</sup>Gal was synthesized as described (18). All other sugar derivatives were purchased from Sigma (St. Louis,

MO). Talon superflow resin was obtained from BD Clontech (Palo Alto, CA). 2-(4'-Maleimidylanilino)naphthalene-6-sulfonic acid (sodium salt) (MIANS) was purchased from Molecular Probes (Eugene, Oregon). All other materials were of reagent grade and were obtained from commercial sources.

**Construction of Mutants.** LacY mutants were constructed by site-specific mutagenesis using the QuikChange II site-directed mutagenesis kit and plasmid pT7-5/LacY as a template. Generally, 30–40 base pair (bp) direct and reverse primers bearing the mutated triplet in the middle of the primer were designed using the Vector NTI 9.1 Suit program (Invitrogen, Carlsbad, CA). All mutagenesis procedures were done according to the QuikChange II manual except that the temperature of the extension reaction was lowered to 68 °C during PCR-directed mutagenesis to reduce possible primer duplication. Mutagenic constructs were sequenced over the entire gene to confirm mutations introduced and to discard unwanted mutations. All constructs were engineered with a C-terminal His-tag to enable purification by affinity chromatography.

**LacY Purification.** LacY mutants were purified from *E. coli* XL1-Blue cells transformed with given plasmids essentially as described (16) by using Co(II) affinity chromatography on Talon resin (BD Clontech, Palo Alto, CA). All protein preparations were at least 95% pure as judged by silver staining after sodium dodecyl sulfate polyacrylamide gel electrophoresis.

**MIANS Labeling.** Purified C154G/V331C/LacY (40–50  $\mu$ M) was labeled with an equimolar concentration of MIANS in 50 mM NaPi (pH 7.0)/0.02% dodecyl- $\beta$ -D-maltopyranoside (DDM) in the presence of 15 mM TDG for protection of Cys148 against alkylation. Reactions were carried out for 15 min at room temperature in the dark. TDG and unreacted MIANS were removed by buffer exchange on an Amicon Ultra-15 concentrator with a 30 kDa cutoff (Millipore, Bedford, MA). The extent of labeling estimated from absorption spectra was 0.7–0.8 mol/mol of protein. Control experiments with C154G/LacY lacking Cys331 resulted in essentially no labeling by MIANS under the same conditions.

**Fluorescence Measurements.** Fluorescence was measured at room temperature with an SLM-Aminco 8100 spectrofluorometer (Urbana, IL) modified for computer-controlled steady-state and stopped-flow modes by OLIS, Inc. (Bogart, GA). Windows-based Olis GlobalWorks software was used for instrument control and stopped-flow trace fitting. All measurements were performed in degassed 50 mM NaPi (pH 7.5)/0.02% DDM. Steady-state measurements were carried out in  $1 \times 1$  cm cuvettes (2 mL) with constant stirring. Emission spectra were recorded with slit widths of 4 and 8 nm for excitation and emission, respectively. All fluorescence changes were corrected for dilution resulting from addition of the ligand. Stopped-flow measurements were performed with an apparatus specifically designed for the SLM-Aminco 8100 by OLIS, Inc. Typically, 0.2 mL solutions from each pneumatically controlled syringe were mixed in a Ball-Berger mixer, and fluorescence changes were recorded using excitation and emission wavelengths of 295 and 330 nm for Trp  $\rightarrow$   $\alpha$ -NPG FRET, respectively, or 330 and 415 nm for MIANS fluorescence, respectively. Binding experiments were carried out by mixing protein samples (syringe 1) with  $\alpha$ -NPG (syringe 2). Displacement rates measurements were done by mixing protein preincubated

with  $\alpha$ -NPG (syringe 1) with an excess of  $\beta$ -D-galactopyranosyl-1-thio- $\beta$ -D-galactopyranoside (TDG) containing the same concentration of  $\alpha$ -NPG as in syringe 1 (syringe 2). The dead time of the instrument (2.7 ms) was determined experimentally by following quenching of *N*-acetyltryptophanamide fluorescence by *N*-bromosuccinimide (19) and was used to correct the measured amplitudes in single-exponential fitting of the fluorescence changes.

**Molecular Modeling.** The X-ray structure of C154G LacY with bound TDG (1PV7) was used for docking of  $\alpha$ -NPG into the sugar-binding site. The coordinates of *p*-aminophenyl- $\alpha$ -D-galactopyranoside bound to enterotoxin B at 1.6 Å resolution (1EFI) were used to build the structure of  $\alpha$ -NPG using Chem3D ultra 9.0 (Chembridgesoft Corp., Cambridge, MA) with energy minimization in the MOPAC module. The resulting coordinates were used for modeling by aligning the galactopyranoside moiety with TDG in the pair-fitting mode (Pymol 0.98, DeLano LLC, Inc.).

## RESULTS

**Modeling of Bound  $\alpha$ -NPG.** LacY contains six Trp residues at positions 10, 33, 78, 151, 171, and 223, five of which are located in N-terminal six-helix bundle. Only Trp151 is in the sugar-binding site located at the apex of the inward-facing cavity in the X-ray structure (Figure 1A). The distance from the indol ring of Trp151 to the furthest galactopyranosyl ring of TDG is about 12 Å, which is favorable for FRET between Trp151 and bound substrate with nitrophenyl or dansyl groups at the anomeric carbon of galactose (20). Indeed, positioning  $\alpha$ -NPG in the sugar-binding site of LacY by aligning the galactopyranosyl ring with TDG places the nitrophenyl moiety about 12 Å from Trp151 (Figure 1B). Therefore, the spatial orientation of  $\alpha$ -NPG in the binding site should yield high efficiency FRET. In contrast, the distance from bound  $\alpha$ -NPG to each of the other five Trp residues is much longer than the Förster distance ( $R_0$ ) for a Trp–nitrobenzoyl pair (16 Å) (20), making FRET unlikely.

**Sugar Binding Determined by Trp  $\rightarrow$   $\alpha$ -NPG FRET.** Initial evidence for FRET between Trp151 and galactopyranosyl derivatives was obtained from steady-state fluorescence experiments. The Trp emission spectrum of C154G/LacY with all six native Trp residues exhibits a maximum at 328 nm (Figure 2A; solid line 1). Addition of increasing concentrations of  $\alpha$ -NPG results in a progressive decrease in Trp fluorescence (Figure 2A; solid lines 2, 3, and 4). Because  $\alpha$ -NPG has a broad absorption spectrum with a maximum at 306 nm (not shown), the sugar derivative affects Trp fluorescence by two simultaneous processes: (1) by serving as a nonfluorescent FRET acceptor from Trp151 in the binding site and (2) by acting as an inner filter and absorbing irradiated excitation light at 295 nm as well as fluorescence emission of Trp. In order to discriminate between the two processes, the relatively high-affinity lactose analogue TDG, which does not absorb light over the range of wavelengths studied, was used. Addition of saturating concentrations of TDG in the absence of  $\alpha$ -NPG causes little or no change in the emission spectrum of Trp (Figure 2A, upper-most broken line). However, when TDG is added after incubation with  $\alpha$ -NPG, a significant increase in Trp fluorescence is observed (Figure 2A, arrows) because of the

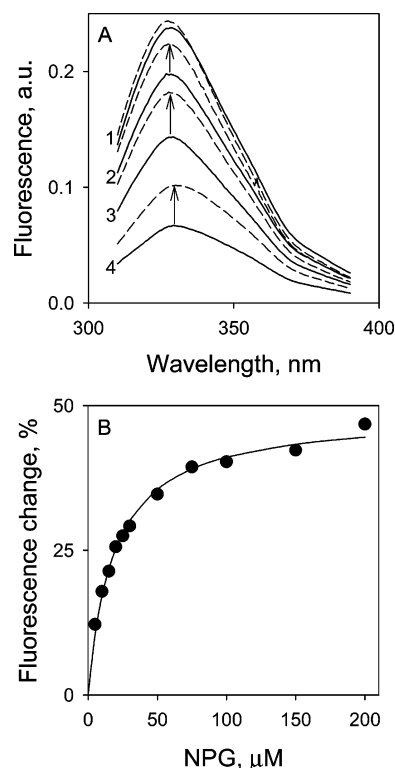


FIGURE 2: Binding of  $\alpha$ -NPG to C154G LacY as detected by Trp  $\rightarrow$   $\alpha$ -NPG FRET. Measurements were carried out in 50 mM NaP<sub>i</sub> (pH 7.5)/0.02% DDM at a protein concentration of 0.4  $\mu$ M; excitation was at 295 nm. (A) Trp emission spectra at different concentrations of  $\alpha$ -NPG. Solid lines represent Trp fluorescence at increasing  $\alpha$ -NPG concentrations: line 1, protein without  $\alpha$ -NPG; line 2, 5  $\mu$ M  $\alpha$ -NPG; line 3, 15  $\mu$ M  $\alpha$ -NPG; line 4, 50  $\mu$ M  $\alpha$ -NPG. Arrows indicate change of fluorescence after displacement of bound  $\alpha$ -NPG by addition of 10 mM TDG. Broken lines indicate spectra after addition of TDG. (B) Affinity of C154G LacY for  $\alpha$ -NPG measured by displacement with TDG. The relative fluorescence change after addition of 10 mM TDG (shown as arrows in panel A) plotted as a function of  $\alpha$ -NPG concentration. Fluorescence after TDG addition was taken as 100% at each  $\alpha$ -NPG concentration. The solid line shows the hyperbolic fit to the data with an estimated  $K_D = 19 \pm 2.0$   $\mu$ M.

displacement of  $\alpha$ -NPG from the binding site. Thus, the increase in Trp fluorescence upon addition of TDG represents a specific FRET effect, and the rest of the fluorescence change that is not restored by TDG represents the nonspecific inner-filter effect (IFE) caused by  $\alpha$ -NPG in solution (21). Specific Trp  $\rightarrow$   $\alpha$ -NPG FRET measured as a result of  $\alpha$ -NPG binding to LacY and displacement by excess of TDG does not involve the nonspecific IFE generated as shown by addition of *p*-nitrophenyl- $\alpha$ -D-glucopyranoside ( $\alpha$ -NPGlc), which does not bind to LacY (22, 23) (see Supporting Information Figure 1S). The apparent affinity for  $\alpha$ -NPG is estimated from the concentration dependence of the specific fluorescence change after addition of excess TDG (Figure 2B). The calculated  $K_D$  of 19  $\mu$ M is virtually identical to that (22 to 32  $\mu$ M) obtained from flow dialysis (15). At a saturating  $\alpha$ -NPG concentration, the maximum change in Trp fluorescence is about 50% (Figure 2B). Thus, the distance between the donor Trp and  $\alpha$ -NPG is close to  $R_0$ , in agreement with the modeling results.

Wild-type LacY exhibits specific Trp  $\rightarrow$   $\alpha$ -NPG FRET in a manner similar to that of mutant C154G/LacY, which binds substrate with high affinity but does very little transport (15, 24, 25). However, the change in Trp fluorescence at



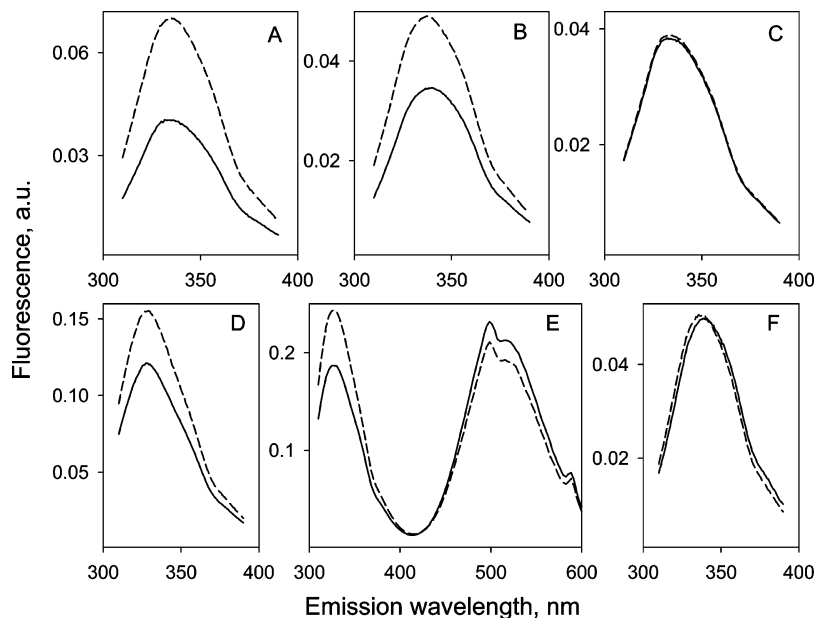


FIGURE 3: Effect of point mutations in LacY and the nature of the sugar on Trp → sugar FRET. Solid lines represent Trp emission spectra (excitation wavelength 295 nm) recorded after short incubation of purified protein in 50 mM NaP<sub>i</sub> (pH 7.5)/0.02% DDM with 100  $\mu$ M sugar derivative prior to TDG addition. Broken lines are Trp emission spectra after addition of 10 mM TDG. The protein concentration was 0.5  $\mu$ M except in panel E where it was 2  $\mu$ M. Trp emission spectra without ligand are not shown. (A) C154G LacY mixed with  $\alpha$ -NPG. (B) Wild-type LacY mixed with  $\alpha$ -NPG. (C) W151Y/C154G LacY mixed with  $\alpha$ -NPG. (D) C154G LacY mixed with *ortho*- $\alpha$ -NPG. (E) C154G LacY mixed with Dns<sup>6</sup>Gal. (F) C154G LacY mixed with  $\alpha$ - or  $\beta$ -NPGlc or with the  $\beta$ -anomer of *para*- or *ortho*-NPG.

the same  $\alpha$ -NPG concentration (100  $\mu$ M) is significantly larger for the C154G mutant relative to that of wild-type LacY (Figure 3A,B, respectively).

Replacement of Trp151 with Tyr completely abolishes Trp →  $\alpha$ -NPG FRET. Trp fluorescence in the presence of  $\alpha$ -NPG is unaffected by addition of TDG (Figure 3C), although both sugars bind to W151Y LacY, as shown by flow dialysis (5). Therefore, it is apparent that Trp151 alone is the FRET donor to  $\alpha$ -NPG; the other five Trp residues do not participate in the phenomenon (compare Figure 3A,C).

The nature of the energy acceptor, as well as the affinity of LacY for the galactosidic substrate, plays an important role in FRET. Addition of the *ortho* derivative of  $\alpha$ -NPG results in significantly less efficient FRET (compare Figure 3A,D), in all likelihood because affinity for *ortho*  $\alpha$ -NPG is 5 times lower than that of the *para* compound (26). Galactopyranosides with nitrophenyl in a  $\beta$ -anomeric configuration exhibit very weak binding (26) and have only a nonspecific inner-filter effect on Trp fluorescence (Figure 3F).

6'-(*N*-Dansyl)aminoethyl-1-thio- $\beta$ -D-galactopyranoside (Dns<sup>6</sup>Gal) is another galactopyranosyl derivative (18) that acts as an acceptor because the  $R_0$  for a Trp–dansyl pair is 21 Å (20). The absorbance maximum of Dns<sup>6</sup>Gal (306 nm) is the same as that of  $\alpha$ -NPG, and it also has a nonspecific inner-filter effect. Unlike  $\alpha$ -NPG, Dns<sup>6</sup>Gal is fluorescent with an emission maximum at 500 nm, thereby allowing detection of FRET as a change in the fluorescence of the donor (Trp), as well as the acceptor (Dns<sup>6</sup>Gal). The data presented in Figure 3E exhibit a simultaneous increase in Trp fluorescence and a decrease in dansyl fluorescence after displacement of bound Dns<sup>6</sup>Gal with excess TDG.

Because the C<sub>4</sub>–OH group of the galactopyranosyl ring determines the specificity of binding (22, 23), *p*-nitrophenyl- $\alpha$ -D-glucopyranoside ( $\alpha$ -NPGlc), which differs from  $\alpha$ -NPG

solely by the position of C<sub>4</sub>–OH in the pyranosyl ring, as well as the  $\beta$ -anomer, was tested. There is no change in Trp fluorescence upon addition of TDG to protein mixed with either sugar (Figure 3F) because neither binds to LacY (23); only the nonspecific inner-filter effect is observed.

**Stopped-Flow Trp151 →  $\alpha$ -NPG FRET.** In order to obtain dynamic information on sugar binding, stopped-flow was applied to measure the time-course of  $\alpha$ -NPG binding. No change in Trp fluorescence is observed when LacY is mixed with buffer alone (Figure 4A, trace 1). Mixing of the protein with increasing concentrations of  $\alpha$ -NPG results in two effects: (1) an initial drop in Trp fluorescence that is proportional to  $\alpha$ -NPG concentration (intercept of traces 2–4 with y axis in Figure 4A), which represents the IFE that cannot be resolved in time by the stopped-flow instrument and (2) a much slower decrease in fluorescence due to Trp →  $\alpha$ -NPG FRET. The traces shown were fitted with a single-exponential equation and corrected for the dead time of the instrument (2.7 ms) (Figure 4, broken lines). Rates of fluorescence change ( $k^{\text{obs}}$ ) increase at higher  $\alpha$ -NPG concentrations (Figure 4A; compare traces 2–4). In contrast, the rate of increase in Trp fluorescence after rapid addition of excess TDG to preformed LacY/ $\alpha$ -NPG complexes is independent of  $\alpha$ -NPG concentration (Figure 4B; compare traces 1 and 2).

The concentration dependence of  $k^{\text{obs}}$  is linear over a wide range of  $\alpha$ -NPG concentrations (Figure 5A). Single-step reversible binding of sugar is a pseudo-first-order reaction when the concentration of protein is much lower than that of the ligand. The reaction can be described as follows:



The  $k^{\text{obs}}$  (reciprocal relaxation time  $1/\tau$ ) for this reaction depends linearly on ligand concentration.

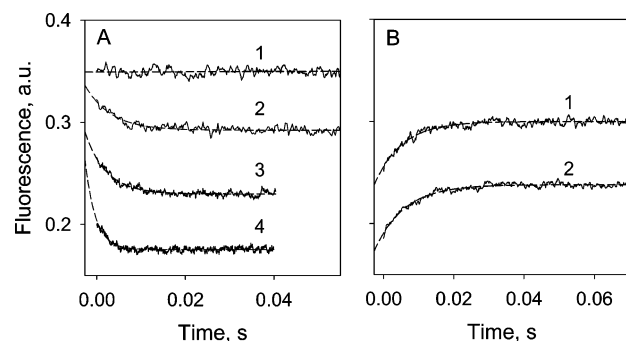


FIGURE 4: Stopped-flow Trp  $\rightarrow$   $\alpha$ -NPG FRET. Trp fluorescence changes with time were recorded after rapid mixing of purified C154G LacY with ligand in 50 mM NaP<sub>i</sub> (pH 7.5)/0.02% DDM. Excitation and emission wavelengths were 295 and 330 nm, respectively. Stopped-flow traces (average of 5–7 measurements shown as solid lines) were fit using a single-exponential equation and corrected for the instrument dead time of 2.7 ms (broken lines). Final protein (1  $\mu$ M) and sugar concentrations are given after mixing. (A) Trp  $\rightarrow$   $\alpha$ -NPG FRET after mixing protein with buffer only (1), 10  $\mu$ M  $\alpha$ -NPG (2), 25  $\mu$ M  $\alpha$ -NPG (3), or 50  $\mu$ M  $\alpha$ -NPG (4). Estimated rates ( $k_{\text{obs}}$ ) are 170, 210, and 420  $\text{s}^{-1}$  for 10, 25, and 50  $\mu$ M  $\alpha$ -NPG, respectively. (B) Displacement of bound  $\alpha$ -NPG by excess TDG. Traces were recorded after mixing a saturating concentration of TDG (15 mM) with protein preincubated with  $\alpha$ -NPG.  $\alpha$ -NPG concentrations were 25 (1) and 50  $\mu$ M (2). Estimated  $k_{\text{obs}}$  are 128 and 122  $\text{s}^{-1}$  for 25 and 50  $\mu$ M  $\alpha$ -NPG, respectively.

$$k_{\text{obs}} = k_{\text{off}} + k_{\text{on}}[\text{S}] \quad (2)$$

The individual rate constants for  $\alpha$ -NPG binding calculated by linear regression analysis are  $k_{\text{on}} = (4.3 \pm 0.2) \times 10^6 \text{ M}^{-1} \text{ s}^{-1}$  (determined from the slope) and  $k_{\text{off}} = 162 \pm 9 \text{ s}^{-1}$  (extrapolation to y axis). The rate of  $\alpha$ -NPG displacement by excess of TDG (open symbol) is in good agreement with  $k_{\text{off}}$  determined from binding experiments (Figure 5A). The equilibrium dissociation constant ( $K_{\text{D}} = k_{\text{off}}/k_{\text{on}}$ ) is  $38 \pm 4 \mu\text{M}$ , in good agreement with the value obtained from steady-state measurements (Figure 2B). The concentration dependence of the amplitude of the fluorescence change taken from the same stopped-flow experiments is shown in Figure 5B. Consistently, the value for  $K_{\text{D}}$  calculated from the data is  $32 \pm 5 \mu\text{M}$ .

**Two-Step Process Detected with MIANS-Labeled LacY.** Replacement of Val331 with Cys allows MIANS labeling at the cytoplasmic end of helix X far from the sugar-binding site (Figure 1A), and sugar binding decreases MIANS fluorescence of labeled single-Cys331 LacY (11, 15, 17). Because Trp  $\rightarrow$   $\alpha$ -NPG FRET measures direct interaction of  $\alpha$ -NPG with LacY, we explored the possibility of comparing the effect of  $\alpha$ -NPG binding on Trp151 and MIANS fluorescence in the same modified protein (i.e., MIANS-labeled V331C/C154G LacY).

MIANS at position 331 is a FRET acceptor from Trp ( $R_0 = 22 \text{ \AA}$ ) (20). Thus, excitation of Trp fluorescence in unlabeled C154G LacY at 295 nm exhibits a typical emission spectrum with a maximum at 330 nm; excitation of MIANS-labeled C154G LacY at 330 nm exhibits MIANS fluorescence with a maximum at 415 nm (Figure 6A, lines 1 and 3, respectively). Dramatically, when the MIANS-labeled protein is excited at 295 nm, Trp fluorescence is markedly diminished, and emission of MIANS at 415 nm is observed. In addition to Trp151, but to a lesser extent, Trp223 may also serve as a FRET donor to MIANS at position 331

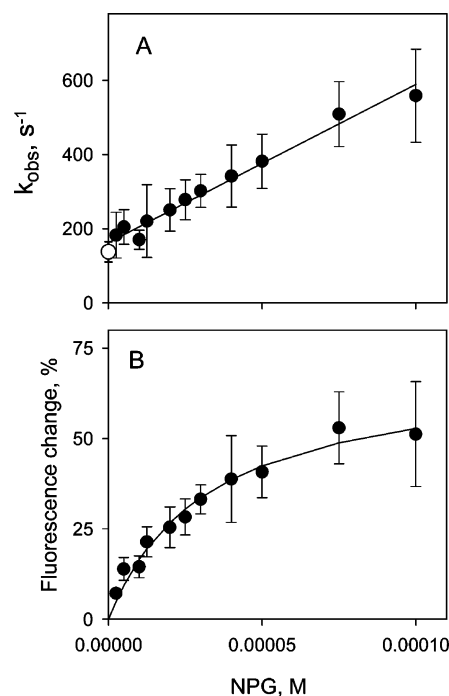


FIGURE 5: Kinetics of  $\alpha$ -NPG binding to C154G LacY detected by Trp  $\rightarrow$   $\alpha$ -NPG FRET. Stopped-flow traces were recorded after rapid mixing of purified protein with given concentrations of  $\alpha$ -NPG, as described in Figure 4 and were individually fitted with a single-exponential equation. Kinetic parameters ( $k_{\text{obs}}$  and amplitude of fluorescence changes) were estimated statistically and plotted versus  $\alpha$ -NPG concentration. Each point is a result of 7–10 measurements with standard deviations shown as vertical bars. (A) Concentration dependence of the rates ( $k_{\text{obs}}$ ) of  $\alpha$ -NPG binding. The open circle represents the rate of displacement of bound  $\alpha$ -NPG (25  $\mu$ M) with 15 mM TDG. The intercept with the y axis is  $k_{\text{off}}$  ( $162 \pm 9 \text{ s}^{-1}$ ), and the slope is  $k_{\text{on}}$  ( $(4.3 \pm 0.2) \times 10^6 \text{ M}^{-1} \text{ s}^{-1}$ ); the estimated  $K_{\text{D}} = 38 \pm 2 \mu\text{M}$ . (B) Concentration dependence of the amplitude of Trp  $\rightarrow$   $\alpha$ -NPG FRET from the experiments shown on panel A. The amplitude of the fluorescence changes at each  $\alpha$ -NPG concentration were corrected for the instrument dead time (2.7 ms) and expressed as percentage of final fluorescence level in each experiment. The solid line is a hyperbolic equation fit to data. Estimated  $K_{\text{D}} = 32 \pm 5 \mu\text{M}$ .

(Figure 1A). However, the remaining four Trp residues in LacY probably play a little role, because the estimated distances between Cys331 and the other four Trp residues are much longer than  $R_0$ . In this regard, the W151Y/V331C LacY mutant labeled with MIANS displays 70–75% less Trp  $\rightarrow$  MIANS FRET, confirming Trp151 as the major donor (data not shown). TDG markedly decreases MIANS emission but has no effect on Trp fluorescence (Figure 6B). Therefore, sugar binding alters the local environment around MIANS at the end of helix X but does not change the distance between Trp151 and MIANS. However, addition of  $\alpha$ -NPG to MIANS-labeled LacY results in significant decreases in both Trp and MIANS fluorescence (Figure 6C).

This complex effect of  $\alpha$ -NPG on fluorescence is a combination of the IFE, Trp  $\rightarrow$   $\alpha$ -NPG FRET, and the specific effect of  $\alpha$ -NPG on MIANS fluorescence, and each effect can be analyzed separately. Stopped-flow traces of the  $\alpha$ -NPG binding were recorded using two sets of wavelengths at each concentration of  $\alpha$ -NPG. Trp  $\rightarrow$   $\alpha$ -NPG FRET was measured at excitation and emission wavelengths of 295 and 330 nm, respectively (Figure 7A), and the decrease in MIANS fluorescence was measured at excitation and emission wavelengths of 330 and 415 nm, respectively (Figure

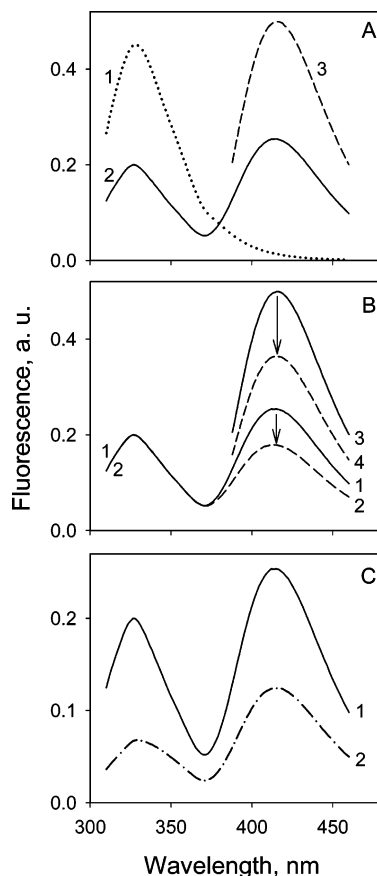


FIGURE 6: Trp  $\rightarrow$   $\alpha$ -NPG FRET and  $\alpha$ -NPG-induced fluorescence change in Mians-labeled C154G/V331C LacY. Emission spectra were recorded in 50 mM NaP<sub>i</sub> (pH 7.5)/0.02% DDM at 0.6  $\mu$ M final protein concentration. (A) Fluorescence of unlabeled (line 1) or Mians-labeled (lines 2 and 3) LacY without sugar; excitation wavelengths 295 nm (lines 1 and 2) or 330 nm (line 3) for Trp  $\rightarrow$   $\alpha$ -NPG FRET or Mians fluorescence, respectively. (B) TDG effect on the fluorescence of Mians-labeled C154G/V331C LacY; excitation at 295 nm (lines 1 and 2) or 330 nm (lines 3 and 4). Solid lines, no TDG; broken lines, addition of 15 mM TDG. The fluorescence change indicated by arrows is 30% in both cases. (C)  $\alpha$ -NPG effect on fluorescence of Mians-labeled LacY with excitation at 295 nm (line 1); no  $\alpha$ -NPG (line 2, addition of 50  $\mu$ M  $\alpha$ -NPG).

7B). Mixing protein with  $\alpha$ -NPG results in two effects: (1) an initial drop of fluorescence caused by the IFE and (2) time-dependent fluorescence changes. Single-exponential fits to the data demonstrate that rates of  $\alpha$ -NPG binding increase with  $\alpha$ -NPG concentration with respect to both Trp  $\rightarrow$   $\alpha$ -NPG FRET and the change in Mians fluorescence but on different time scales (compare traces 1–3 in Figure 7A,B). The rate of change in Mians fluorescence is clearly slower than the rate of change in Trp  $\rightarrow$   $\alpha$ -NPG FRET at given  $\alpha$ -NPG concentrations. Furthermore, the rate of  $\alpha$ -NPG displacement with a saturating concentration of TDG measured for Mians-labeled protein is in good agreement with the rate of sugar release for protein unmodified with Mians (compare upper trace on Figures 7A and 4B).

The concentration dependence for the rate change in fluorescence measured at 330 (Trp  $\rightarrow$   $\alpha$ -NPG FRET) and 415 nm (Mians) in the same stopped-flow experiment is very different (Figure 8A,B). Trp  $\rightarrow$   $\alpha$ -NPG FRET displays a linear dependence on  $\alpha$ -NPG concentration (Figure 8A) in essentially the same manner as for LacY unmodified with Mians (Figure 5A). In contrast, the rate change in Mians

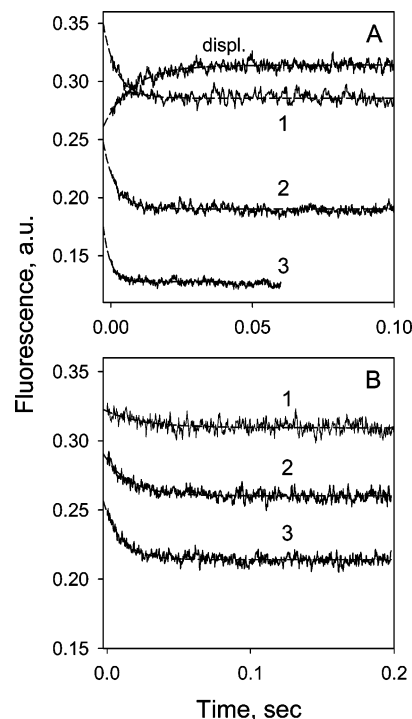


FIGURE 7: Time-dependent changes in Trp  $\rightarrow$   $\alpha$ -NPG FRET (A) or Mians fluorescence (B) with Mians-labeled C154G/331C LacY. Stopped-flow traces were recorded after rapid mixing of protein (1  $\mu$ M, final concentration) with  $\alpha$ -NPG at excitation and emission wavelengths of 295 and 330 nm (A) or 330 and 415 nm (B), respectively.  $\alpha$ -NPG concentrations were 20  $\mu$ M (1), 50  $\mu$ M (2), or 100  $\mu$ M (3). The upper trace in panel A represents displacement of bound  $\alpha$ -NPG (25  $\mu$ M) by an excess of TDG (15 mM). Other experimental details are described in Figure 4. Estimated rates ( $k_{\text{obs}}$ ) are 210, 230, and 380  $\text{s}^{-1}$  for traces 1, 2, and 3 in panel A, and 40, 58, and 82  $\text{s}^{-1}$  for traces 1, 2, and 3 in panel B, respectively.

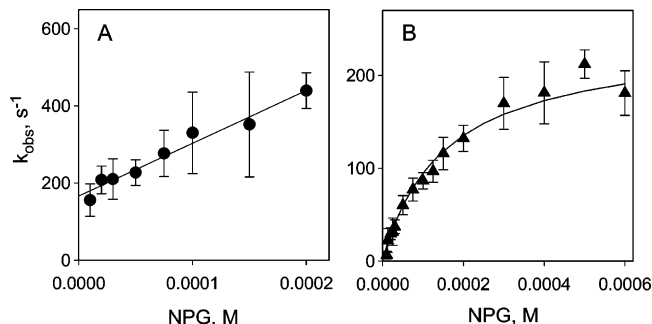
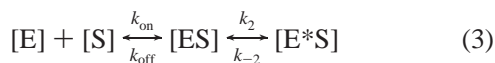


FIGURE 8: Concentration dependence of the rates of Trp  $\rightarrow$   $\alpha$ -NPG FRET (A) and  $\alpha$ -NPG-induced changes in Mians fluorescence (B) with Mians-labeled C154G/V331C LacY. Two sets of data were collected after mixing of Mians-labeled protein with  $\alpha$ -NPG by stopped-flow. (A) excitation and emission wavelengths, 295 and 330 nm for Trp  $\rightarrow$   $\alpha$ -NPG FRET. (B) excitation and emission wavelengths, 330 and 415 nm for Mians fluorescence. Other experimental details are described in the legend to Figure 5. The solid line in panel A shows linear regression fit with  $k_{\text{off}} = 166 \pm 10 \text{ s}^{-1}$  and  $k_{\text{on}} = (1.4 \pm 0.1) \times 10^6 \text{ M}^{-1} \text{ s}^{-1}$ . Estimated  $K_D = 121 \pm 8 \text{ } \mu\text{M}$ . The solid line in panel B shows the hyperbolic fit (eq 4) to the experimental data with estimated parameters  $k_2 = 238 \pm 12 \text{ s}^{-1}$ ,  $k_{-2} = 2 \pm 7 \text{ s}^{-1}$ , and  $K_D = 158 \pm 31 \text{ mM}$ .

fluorescence exhibits a hyperbolic dependence on  $\alpha$ -NPG concentration (Figure 8B), indicating that there are at least two steps in the overall process.

A two-step reversible reaction can be described as follows:





The observed rate  $k_1^{\text{obs}}$  ( $1/\tau_1$ ) for the first step ( $\text{Trp} \rightarrow \alpha\text{-NPG}$  FRET) depends linearly on ligand concentration (Figure 8A), and the kinetic parameters  $k_{\text{on}}$  and  $k_{\text{off}}$  are estimated from linear regression analyses (eq 2). The observed rate  $k_2^{\text{obs}}$  ( $1/\tau_2$ ) for the second step (the change in MANS fluorescence) exhibits a hyperbolic dependency on the concentration of the substrate (Figure 8B), indicating that the second step is slow, with forward and reverse rate constants ( $k_2$  and  $k_{-2}$ ) estimated from eq 4 (27):

$$k_2^{\text{obs}} = k_{-2} + k_2[S]/([S] + K_D) \quad (4)$$

The calculated values of  $k_{\text{on}}$  and  $k_{\text{off}}$  for  $\text{Trp} \rightarrow \alpha\text{-NPG}$  FRET with MANS-labeled protein are  $(1.4 \pm 0.1) \times 10^6 \text{ M}^{-1} \text{ s}^{-1}$  and  $166 \pm 10 \text{ s}^{-1}$ , respectively. The binding affinity for  $\alpha\text{-NPG}$  is 3–4 times lower for the MANS-modified protein ( $K_D = 120 \pm 8 \mu\text{M}$ ) because  $k_{\text{on}}$  is ca. 3 times lower than that observed for the unlabeled protein (see Figure 5A). The  $K_D$  calculated from the hyperbolic concentration dependence of the rate change in MANS fluorescence ( $158 \pm 31 \mu\text{M}$ ) is consistent with the  $K_D$  calculated from  $k_{\text{on}}$  and  $k_{\text{off}}$  derived from the  $\text{Trp} \rightarrow \alpha\text{-NPG}$  FRET measurements. The values of  $k_2$  and  $k_{-2}$  calculated from eq 4 are  $238 \pm 12$  and  $2.3 \pm 7.5 \text{ s}^{-1}$ , respectively.

## DISCUSSION

Modeling studies (Figure 1B) indicating that  $\alpha\text{-NPG}$  should act as a FRET acceptor from Trp are confirmed by fluorescence experiments. Trp fluorescence decreases dramatically upon addition of  $\alpha\text{-NPG}$  in two phases, a nonspecific filter effect and a specific FRET signal that is elicited in steady-state experiments by displacement of the acceptor  $\alpha\text{-NPG}$  with TDG, a nonfluorescent galactopyranoside (Figure 2A). The apparent affinity for  $\alpha\text{-NPG}$  calculated from the concentration dependence (Figure 2B) is very similar to that measured by flow dialysis (15). Wild-type LacY also exhibits  $\text{Trp} \rightarrow \alpha\text{-NPG}$  FRET but with lower efficiency (Figure 3B), which is consistent with the lower affinity of the wild-type protein for  $\alpha\text{-NPG}$ . Replacement of Trp151 with Tyr results in a complete loss of the specific FRET effect, although the mutation does not preclude substrate binding (5–7). The observation strongly indicates that the other five Trp residues in LacY do not participate in  $\text{Trp} \rightarrow \alpha\text{-NPG}$  FRET and that Trp151 is the only energy donor, as predicted from the structure and modeling, thereby obviating the need for single-Trp151.

Mutant C154G in the membrane binds ligand at least as well as wild-type LacY but is defective with respect to all modes of sugar translocation (15, 24, 25). In addition, purified C154G LacY binds  $\alpha\text{-NPG}$  with 2–3 times better affinity than wild-type, exhibits little tendency to aggregate in DDM, is thermostable, and strongly favors an inward-facing conformation (1PV7) (4, 15, 16). In these experiments, C154G LacY was used in order to study a well-expressed, stable molecule that binds  $\alpha\text{-NPG}$  with high affinity, which reduces the inner-filter effect.

Only galactoside derivatives that have an absorption overlapping with the Trp emission wavelength are acceptors for energy transfer. The galactopyranosyl ring is the specific-

ity determinant for binding to LacY, and affinity depends on the nature of the sugar homologue. Thus, glucopyranosides, which differ from galactopyranosides only by the orientation of the  $\text{C}_4\text{-OH}$ , do not bind (22, 23) and have no specific effect on Trp fluorescence (Figure 3F). Furthermore, hydrophobic aglycons of D-galactopyranosides increase binding affinity, and  $\alpha$  anomers have higher affinity than  $\beta$  anomers (26). Consistently, the largest specific FRET signal is observed with  $\alpha\text{-NPG}$ , and the  $\beta$  anomer of either *para*- or *ortho*-NPG causes no specific change whatsoever in Trp fluorescence (Figure 3F). However, other nitrophenyl derivatives such as *ortho*- $\alpha\text{-NPG}$  and Dns<sup>6</sup>Gal also exhibit FRET (Figure 3D,E). Moreover, with Dns<sup>6</sup>Gal binding to LacY, FRET monitored by a TDG-induced increase in Trp fluorescence coincides with a reciprocal decrease in Dns<sup>6</sup>Gal fluorescence due to Dns<sup>6</sup>Gal displacement (Figure 3E).

Steady-state  $\text{Trp} \rightarrow \alpha\text{-NPG}$  FRET at increasing concentrations of  $\alpha\text{-NPG}$  yields an apparent  $K_D$  for  $\alpha\text{-NPG}$  but gives no information regarding rates of binding or release. However, time-dependent  $\text{Trp} \rightarrow \alpha\text{-NPG}$  FRET obtained by stopped-flow allows direct determination of sugar binding rates. Thus, an important step in the overall mechanism of LacY, ligand binding, can be studied by measuring the kinetic parameters for  $\alpha\text{-NPG}$  binding.

Rates of sugar binding were measured at  $\alpha\text{-NPG}$  concentrations ranging 5–100  $\mu\text{M}$ . The fluorescence change with time is a pseudo-first-order process, and the data fit well to a single-exponential. The effect of  $\alpha\text{-NPG}$  concentration on the rate of binding is linear (Figure 5A), as predicted by eq 2, indicating that the phenomenon represents a single step in the transport mechanism. Estimated individual rate constants for  $\alpha\text{-NPG}$  binding are  $k_{\text{on}} = 4.3 \times 10^6 \text{ M}^{-1} \text{ s}^{-1}$  and  $k_{\text{off}} = 162 \text{ s}^{-1}$ . The equilibrium dissociation constant for  $\alpha\text{-NPG}$  binding in DDM calculated from individual rate constants is 38  $\mu\text{M}$ , which is virtually identical to the  $K_D$  calculated from the stopped-flow fluorescence amplitude change (Figure 5B) and from steady-state measurements (Figure 2B) as well as that obtained with flow dialysis (15).

The X-ray structure of the C154G mutant with bound TDG (1PV7) and wild-type LacY are in an inward-facing conformation. However, the  $K_D$  ligand is the same on both sides of the membrane within experimental error (28). The rate constants estimated from stopped flow ( $k_{\text{on}} = 4.3 \times 10^6 \text{ M}^{-1} \text{ s}^{-1}$ ;  $k_{\text{off}} = 162 \text{ s}^{-1}$ ) are considerably faster than the turnover number for LacY (30–50  $\text{s}^{-1}$ ) (29). The sugar-binding site in LacY is exposed only to the cytoplasmic side of the molecule, and the periplasmic side is completely blocked (3, 4, 9). Therefore, although the results presented here might be interpreted superficially to indicate that accessibility of the binding site is not a rate-limiting step in the transport mechanism, these experiments were carried out in detergent where accessibility to the sugar-binding site is not a consideration. Therefore, if the inward-facing conformation is the lowest free energy conformation of LacY in the membrane, it is possible that accessibility of the binding site to the periplasmic side of the membrane is rate-limiting for transport.

V331C LacY labeled with MANS at Cys331 is a model for studying the effect of a sugar-induced conformational change. The residues in LacY involved in galactopyranoside-specific binding are located within the N-terminal six-helix bundle, and Cys331 is on helix X in the C-terminal six-helix

bundle, which contains several amino acid residues required for  $H^+$  translocation. Stopped-flow measurements of fluorescence changes induced by  $\alpha$ -NPG with MIANS-labeled V331C LacY provide a unique opportunity to measure rates of binding ( $Trp \rightarrow \alpha$ -NPG FRET), as well as rates of conformational change reflected by MIANS in the same protein sample. It is noteworthy that rates of binding measured by  $Trp \rightarrow \alpha$ -NPG FRET ( $k_1^{obs}$ ) vary linearly with sugar concentration for unmodified and MIANS-labeled LacY (Figures 8A and 5A). The calculated  $k_{on}$  for MIANS-labeled protein is about 3 times lower when compared with that of the unmodified protein, which alters  $\alpha$ -NPG affinity proportionally, because  $k_{off}$  is similar in both cases. A reasonable explanation is that modification of V331C by MIANS positions the bulky fluorophore in the vicinity of the inward-facing cavity, thereby limiting access of ligand to the binding site. The hyperbolic dependence of the change in MIANS fluorescence on  $\alpha$ -NPG concentration ( $k_2^{obs}$ ) is a strong indication that relatively rapid formation of the protein–sugar complex is followed by a slower conformational change (27). Moreover, it is likely that the sugar-induced change in MIANS fluorescence is related to the global conformational change that occurs during transport, because the phenomenon occurs much more rapidly in the absence of the C154G mutation (I.N.S., V.N.K., and H.R.K., unpublished observations).

Finally, the findings presented here are consistent with recent observations regarding the thermodynamics of ligand-induced changes in the conformation of wild-type and C154G LacY, as studied by isothermal calorimetry.<sup>30</sup> The change in free energy upon  $\alpha$ -NPG binding is similar for wild-type LacY or the C154G mutant. However, with the wild-type, the change in free energy upon binding is due primarily to an increase in entropy; in marked contrast, an increase in enthalpy is solely responsible for the change in free energy in the mutant. Thus, wild-type LacY behaves as if there are multiple ligand-bound conformational states, and the mutant is severely restricted.

## ACKNOWLEDGMENT

We are indebted to Tatsushi Toyokuni and Paula Gunawan for synthesizing Dns<sup>6</sup>Gal.

## SUPPORTING INFORMATION AVAILABLE

$Trp \rightarrow \alpha$ -NPG FRET graphs. This material is available free of charge via the Internet at <http://pubs.acs.org>.

## REFERENCES

- Saier, M. H., Jr., Beatty, J. T., Goffeau, A., Harley, K. T., Heijne, W. H., Huang, S. C., Jack, D. L., Jahn, P. S., Lew, K., Liu, J., Pao, S. S., Paulsen, I. T., Tseng, T. T., and Virk, P. S. (1999) The major facilitator superfamily, *J. Mol. Microbiol. Biotechnol.* **1**, 257–279.
- Kaback, H. R., Sahin-Toth, M., and Weinglass, A. B. (2001) The kamikaze approach to membrane transport, *Nat. Rev. Mol. Cell. Biol.* **2**, 610–620.
- Guan, L., and Kaback, H. R. (2006) Lessons from Lactose Permease, *Annu. Rev. Biophys. Biomol. Struct.* **35**, 67–91.
- Abramson, J., Smirnova, I., Kasho, V., Verner, G., Kaback, H. R., and Iwata, S. (2003) Structure and mechanism of the lactose permease of *Escherichia coli*, *Science* **301**, 610–615.
- Guan, L., Hu, Y., and Kaback, H. R. (2003) Aromatic stacking in the sugar binding site of the lactose permease, *Biochemistry* **42**, 1377–1382.
- Vazquez-Ibar, J. L., Guan, L., Svrakic, M., and Kaback, H. R. (2003) Exploiting luminescence spectroscopy to elucidate the interaction between sugar and a tryptophan residue in the lactose permease of *Escherichia coli*, *Proc. Natl. Acad. Sci. U.S.A.* **100**, 12706–12711.
- Vazquez-Ibar, J. L., Guan, L., Weinglass, A. B., Verner, G., Gordillo, R., and Kaback, H. R. (2004) Sugar Recognition by the Lactose Permease of *Escherichia coli*, *J. Biol. Chem.* **279**, 49214–49221.
- Weinglass, A., Whitelegge, J. P., Faull, K. F., and Kaback, H. R. (2004) Monitoring Conformational Rearrangements in the Substrate-binding Site of a Membrane Transport Protein by Mass Spectrometry, *J. Biol. Chem.* **279**, 41858–41865.
- Mirza, O., Guan, L., Verner, G., Iwata, S., and Kaback, H. R. (2004) Structural evidence for induced fit and a mechanism for sugar/H(+) symport in LacY, *Embo J.* **25**, 1177–1185.
- Rudnick, G., Schuldiner, S., and Kaback, H. R. (1976) Equilibrium between two forms of the *lac* carrier protein in energized and nonenergized membrane vesicles from *Escherichia coli*, *Biochemistry* **15**, 5126–5131.
- Wu, J., Frillingos, S., Voss, J., and Kaback, H. R. (1994) Ligand-induced conformational changes in the lactose permease of *Escherichia coli*: evidence for two binding sites, *Protein Sci.* **3**, 2294–2301.
- Frillingos, S., and Kaback, H. R. (1996) Probing the conformation of the lactose permease of *Escherichia coli* by in situ site-directed sulfhydryl modification, *Biochemistry* **35**, 3950–3956.
- Sahin-Toth, M., Karlin, A., and Kaback, H. R. (2000) Unraveling the mechanism of lactose permease of *Escherichia coli*, *Proc. Natl. Acad. Sci. U.S.A.* **97**, 10729–10732.
- le Coutre, J., Whitelegge, J. P., Gross, A., Turk, E., Wright, E. M., Kaback, H. R., and Faull, K. F. (2000) Proteomics on full-length membrane proteins using mass spectrometry, *Biochemistry* **39**, 4237–4242.
- Smirnova, I. N., and Kaback, H. R. (2003) A Mutation in the Lactose Permease of *Escherichia coli* That Decreases Conformational Flexibility and Increases Protein Stability, *Biochemistry* **42**, 3025–3031.
- Ermolova, N. V., Smirnova, I. N., Kasho, V. N., and Kaback, H. R. (2005) Interhelical packing modulates conformational flexibility in the lactose permease of *Escherichia coli*, *Biochemistry* **44**, 7669–7677.
- Venkatesan, P., and Kaback, H. R. (1998) The substrate binding site in the lactose permease of *Escherichia coli*, *Proc. Natl. Acad. Sci. U.S.A.* **95**, 9802–9807.
- Schuldiner, S., Kerwar, G. K., Kaback, H. R., and Weil, R. (1975) Energy-dependent binding of dansylgalactosides to the  $\beta$ -galactoside carrier protein, *J. Biol. Chem.* **250**, 1361–1370.
- Peterman, B. F. (1979) Measurement of the dead time of a fluorescence stopped-flow instrument, *Anal. Biochem.* **93**, 442–444.
- Wu, P., and Brand, L. (1994) Resonance energy transfer: methods and applications, *Anal. Biochem.* **218**, 1–13.
- Puchalski, M. M., Morra, M. J., and von Wandruszka, R. (1991) Assessment of corrections for the inner filter effect in fluorimetry, *Fresenius J. Anal. Chem.* **340**, 341–344.
- Sahin-Toth, M., Akhoon, K. M., Runner, J., and Kaback, H. R. (2000) Ligand recognition by the lactose permease of *Escherichia coli*: specificity and affinity are defined by distinct structural elements of galactopyranosides, *Biochemistry* **39**, 5097–5103.
- Sahin-Toth, M., Lawrence, M. C., Nishio, T., and Kaback, H. R. (2001) The C-4 hydroxyl group of galactopyranosides is the major determinant for ligand recognition by the lactose permease of *Escherichia coli*, *Biochemistry* **40**, 13015–13019.
- Menick, D. R., Sarkar, H. K., Poonian, M. S., and Kaback, H. R. (1985) Cys154 is important for *lac* permease activity in *Escherichia coli*, *Biochem. Biophys. Res. Commun.* **132**, 162–170.
- van Iwaarden, P. R., Driessen, A. J., Lolkema, J. S., Kaback, H. R., and Konings, W. N. (1993) Exchange, efflux, and substrate binding by cysteine mutants of the lactose permease of *Escherichia coli*, *Biochemistry* **32**, 5419–5424.
- Sahin-Toth, M., Gunawan, P., Lawrence, M. C., Toyokuni, T., and Kaback, H. R. (2002) Binding of hydrophobic D-galactopyranosides to the lactose permease of *Escherichia coli*, *Biochemistry* **41**, 13039–13045.
- Fersht, A. (1999) *Structure and mechanism in Protein Science: a guide to enzyme catalysis and protein folding*, W. H. Freeman, New York.



28. Guan, L., and Kaback, H. R. (2004) Binding affinity of lactose permease is not altered by the  $H^+$  electrochemical gradient, *Proc. Natl. Acad. Sci. U.S.A.* 101, 12148–12152.
29. Viitanen, P., Garcia, M. L., and Kaback, H. R. (1984) Purified reconstituted lac carrier protein from *Escherichia coli* is fully functional, *Proc. Natl. Acad. Sci. U.S.A.* 81, 1629–1633.
30. Nie, Y., Smirnova, I., Kasho, V., and Kaback, H. R. (2006) Energetics and Ligand-Induced Conformational Flexibility in the Lactose Permease of *Escherichia Coli*, *J. Biol. Chem.* 281, 35779–35784.

BI061632M